

Inorg Chem. Author manuscript; available in PMC 2014 May 20.

Published in final edited form as:

Inorg Chem. 2013 May 20; 52(10): 5642–5644. doi:10.1021/ic4005938.

Electronic Structural Changes of Mn in the Oxygen-Evolving Complex of Photosystem II During the Catalytic Cycle

Pieter Glatzel^{1,*}, Henning Schroeder², Yulia Pushkar^{2,†}, Thaddeus Boron III³, Shreya Mukherjee⁴, George Christou⁴, Vincent L. Pecoraro³, Johannes Messinger⁵, Vittal K. Yachandra^{2,*}, Uwe Bergmann^{6,*}, and Junko Yano^{2,*}

¹European Synchrotron Radiation Facility, Grenoble, France

²Physical Biosciences Division, Lawrence Berkeley National Laboratory, Berkeley, CA

³Dept. of Chemistry, Univ. of Michigan, Ann Arbor, MI

⁴Dept. of Chemistry, Univ. of Florida, Gainesville, FL

⁵Institutionen för Kemi, Kemiskt Biologiskt Centrum, Umeå Universitet, Umeå, Sweden

⁶LCLS, SLAC National Accelerator Laboratory, Menlo Park, CA

Abstract

The oxygen evolving complex (OEC) in Photosystem II (PS II) was studied in the S_0 through S_3 states using 1s2p direct resonant inelastic X-ray scattering (RIXS) spectroscopy. The spectral changes of the OEC during the S-state transitions are subtle, indicating that the electrons are strongly delocalized throughout the cluster. The result suggests that in addition to the Mn ions ligands are also playing an important role in the redox reactions. A series of M^{IV} coordination complexes with different protonation states, nuclearity, and with and without the presence of Ca were compared, particularly with the PS II S_3 state spectrum to understand its oxidation state. We find strong variations of the electronic structure within the series of M^{IV} model systems. The spectrum of the S_3 state best resembles the M^{IV} complexes, M^{IV} Ca2 and sapln M^{IV} (OH)2, *i.e.* the oxo-bridge protonation of Mn dimer complexes and the presence of Ca in one corner of a Mn cubane structure show a similar spectroscopic response, suggesting that Ca in PS II and protonation of the oxo-bridge may give rise to analogous modifications of the electronic structure at the Mn sites. The current result emphasizes that the assignment of formal oxidation states alone is not sufficient for understanding the detailed electronic structural changes that govern the catalytic reaction in the OEC.

The oxygen-evolving complex (OEC) located in the Photosystem II (PS II) membrane-bound protein in plants, algae, and cyanobacteria catalyzes the water-oxidation reaction. 1 The OEC, an oxo-bridged complex of four Mn and one Ca ions (Mn₄CaO₅ cluster), couples the 4-electron chemistry of water oxidation with the one-electron photochemistry of the reaction center by sequentially storing oxidizing equivalents through five intermediate S-states (S_i, i = 0 to 4), before one molecule of dioxygen is evolved. The Mn₄CaO₅ cluster provides a high degree of redox and chemical flexibility so that several oxidizing equivalents can be stored during the S-state cycle. To understand the mechanism of water

Department of Physics, Purdue University, 525 Northwestern West Lafayette, Indiana, 47907, USA.

oxidation in detail, it is crucial to understand the changes of the electronic structure in the OEC over the whole course of the catalytic cycle.²

There is a consensus that Mn-centered oxidation occurs during the S_0 to S_1 , and S_1 to S_2 transitions. However, there has been a long debate regarding the nature of the S_2 to S_3 transition. Within the context of localized oxidation, the formal oxidation state of the native S_1 state has been assigned to $Mn_2^{III}Mn_2^{IV}$ and S_2 to $Mn^{III}Mn_3^{IV}$. In the S_0 state, involvement of Mn^{II} has been discussed, while recent ENDOR studies³ support the formal oxidation state of $Mn_3^{III}Mn^{IV}$. In the S_3 state, the question remains whether a Mn-centered oxidation occurs⁴ and therefore all Mn become Mn^{IV} , or a ligand-centered oxidation takes place before O-O bond formation and release of molecular oxygen.⁵ This incomplete understanding of the S_2 to S_3 transition has led to two different types of proposed O_2 evolution mechanisms, with one type incorporating the nucleophilic attack mechanism of high-valent Mn, and the other involving oxo-radicals.^{2, 6} Fundamental differences in the chemistry of O-O bond formation and O_2 evolution exist between the two types of mechanisms.

In our earlier RIXS study it was shown that the electron in the S_1 to S_2 transition is removed from a strongly delocalized orbital, indicating strong covalency within the Mn_4CaO_5 cluster and that the oxidation therefore cannot be assigned to just one Mn atom in the OEC. In the current study, we present RIXS data on PS II from S_0 through the S_3 states of the OEC. We compared the S_3 spectrum with model compounds, where Mn has the formal oxidation state IV, with different nuclearities, types of ligands, and geometries.

In 1s2p RIXS spectroscopy (Scheme 1), a Mn 1s electron is excited into the lowest unoccupied molecular orbitals (LUMOs). The orbitals have mainly Mn 3d character mixed with Mn 4p and ligand orbitals. The electronic configuration can be approximated by $1s^13d^{n+1}$ and the spectral features are the K absorption pre-edge. The excited states decay and release a photon whose energy is recorded in order to obtain the energy that remains in the sample (energy transfer). The most probable transition is 2p to 1s to reach the final state configuration $2p^53d^{n+1}$, which is formally identical to that of L-edge spectroscopy. The creation of inner-shell electron vacancies renders this technique element-selective and sensitive to both the metal ion charge and spin density.

RIXS spectra are shown as a two-dimensional contour plots (*c.f.* Figure 1) with incident energy and energy transfer along the axes. The spectral broadening along the energy transfer axis is not governed by the short core hole lifetime of the intermediate state, but the longer lived final state, resulting in sharp spectral features. Thus, RIXS spectroscopy considerably improves the pre-edge separation from the main edge feature as compared to XAS in which it is usually difficult to distinguish the contribution of strong main edge transition (seen as strong rising intensity in the highest energy region in Fig. 1). The main spectral features extend along a diagonal streak in the 1s2p RIXS plane. Spectral features off this diagonal line result from different interactions of the 1s and the 2p core hole with the valence electrons. These direct Coulomb and exchange interactions are considerably stronger for a 2p core hole, making the technique also sensitive to the spin density of Mn.

Figure 1 shows RIXS spectra of PS II in the S_0 to S_3 states and a series of Mn model complexes. The 1s2p RIXS planes of Mn^{IV} systems (Fig. 1b–h, chemical structures of b–g shown in SI) vary significantly, demonstrating that a Mn^{IV} species does not provide a single unique spectroscopic fingerprint. The spectral shape is strongly influenced by the local density of unoccupied electronic states. The K absorption pre-edges obtain spectral intensity from electric dipole and quadrupole transitions depending on the local symmetry. Therefore, the spectral intensity may vary considerably depending on the number and type of ligands.⁸

The coordination complexes in Fig. 1 all have six-coordinated Mn and the ratio between dipole and quadrupole contribution to the pre-edge will vary little. We attribute intensity variations to modifications in the composition of the molecular orbitals.

The overall trend observed in the 1s2p RIXS planes is a shift of spectral intensity to higher energies with increasing positive charge on the metal. The solid state system $Mn^{IV}O_2$ (Fig. 1h) has its highest energy peak at 6542.9 eV, representing the most ionic form of Mn^{IV} possibly induced by the extended structure of the Mn-O lattice. The Mn^{IV} coordination complexes (Fig. 1b–g)⁹ are distinctly different from the oxides. They show three main spectral features in the energy range of 6539-6544 eV. The low energy feature at 6541 eV (indicated as 1 in Fig. 1b) is sharper than the structures at higher energies. It corresponds to the excitations of 1s electron into LUMOs that are localized, and therefore exhibit a more atomic character. The effect of the ligand environment becomes more dominant towards higher energies (6541-6544 eV, indicated as 2 in Fig. 1b), resulting in broader spectral features due to the orbital splittings. The intensity around 6542 eV appears off-diagonal (indicated as 3 in Fig. 1b), shifted towards higher energy transfer which is caused by strong (2p,3d) electron-electron interactions.

A series of di- μ -oxo bridged Mn salpn compounds (salpn₂Mn₂IV(OH)₂, salpn₂Mn₂IVOOH, and salpn₂Mn₂IVO₂, Fig. 1 b–d) demonstrates the sensitivity of 1s2p RIXS to the sequential protonation of the bridging oxygen. They show a transfer of spectral intensity from low to the high energy features. Replacing OH⁻ with O²⁻ thus results in a 1s2p RIXS plane with the spectral weight predominantly in the region where also Mn^{IV}O₂ (Fig. 1h) shows its strongest spectral feature.

The spectra of $Mn_3^{IV}O_4$ Acbpy (Fig. 1g), salpn₂Mn₂^{IV}O₂ (Fig. 1d), and phen₄Mn₂^{IV}O₂ (Fig. 1e) show maximum intensity at higher energies (6541 – 6544 eV) as opposed to other compounds (e.g. Figs. 1b, f). In all cases the di- μ -oxo bridge is not protonated. This confirms that the bridging ligand including its degree of protonation has a strong influence on the electronic structure around Mn. The subtle differences at higher energies observed among the three compounds reflect the orbital modifications at the Mn sites when replacing N with O (SI Fig. S1) and slightly changing the bond distances and angles. $Mn_3^{IV}O_4$ Acbpy (Fig. 1g) with two di- μ -oxo bridges and additonal O ligands have their main peak intensity at higher energy. The phen₄Mn₂IVO₂ complex (Fig. 1e) with N ligands and two di- μ -oxo bridges, by contrast, shows spectral intensity at lower energies than salpn₂Mn₂IVO₂ (Fig. 1d) where each Mn has two additional O ligands. The spectrum of Mn₃Ca₂ (Fig. 1f) resembles salpn₂Mn₂IV(O)(OH) with single protonation of the oxo-bridge (Fig. 1c). The Mn₃Ca₂ compound contains a cubane-like structure that consists of a Mn₃IVCaO₄ moiety. The presence of Ca within the cubane-like structure appears to modify the electronic structure of Mn in a similar way as we observe for protonation of the oxo-bridge.

Pure S_0 , S_1 , S_2 , and S_3 spectra shown in Figs. 1 and 2 were obtained by the deconvolution of the flash illuminated samples using the calculated S-state distribution from EPR (see SI, Fig. S2a–c). Within the series of PS II data we observe a small shift of spectral intensity to higher energies between S_0 and S_3 confirming the oxidation at the Mn sites during the catalytic cycle.⁷ This is also observed in the XAS pre-edge spectra as shown in Fig. 2. A low energy shoulder appears in the S_0 pre-edge spectrum which is seen as a low energy component in the RIXS S_0 spectrum (Fig. 1). Upon the S_0 to S_1 transition, the low energy shoulder in the pre-edge spectra (Fig. 2) becomes weaker and the spectrum can be fitted with two strong components (~6541.1 and ~6542.8 eV) in the S_1 to S_3 states. Note that the instrumental resolution for the PS II RIXS data in Fig. 1 is lower compared to the model compounds because the data were recorded at different experimental stations. However, the striking observation when comparing PS II and model compound data is that the spectral

changes during the PS II catalytic cycle (Fig. 1) are considerably weaker than the spectral differences among the Mn^{IV} coordination complexes.

In the S₀ state, two different formal oxidation states, II,III,IV₂ and III₃,IV, have been proposed from the previous EPR¹⁰, XANES⁵ and other studies. Recent ⁵⁵Mn ENDOR studies³ have shown that the data are compatible with the formal oxidation state of III₃,IV. In RIXS, Mn^{II} compounds show a characteristic feature due to the strong stabilizing energy of a 3d⁵ S valence shell configuration at around ~6540 eV. Unlike Mn^{IV} model compounds, Mn^{II} in both the oxide (Mn^{II}O, Fig. 1a) and coordination complexes (not shown here) have very similar spectral features. In the S₀ state, both RIXS and XAS data show spectral intensity at low energies (~6540 eV), which could indicate a contribution of Mn^{II}. This low energy component becomes weak in the S_0 to S_1 transition. However, Mn^{III} compounds may also show a low energy feature around ~6540 eV that originates from strong (3d, 3d) electron-electron interactions. Therefore, a comparison of the RIXS S₀ spectrum with Mn^{II}O (Fig. 1a) does not confirm the presence or absence of Mn^{II} in the S₀ state. This would require a considerably larger set of experimental data combined with quantum chemical calculations of the spectra. The latter is currently not possible with the required accuracy due to the complexity of 3d³ and 3d⁴ systems, because the pre-edge is shaped by electric dipole and quadrupole transitions, and the current limitation of quantum chemical codes to include fully the core hole effect.

A comparison of the S_3 RIXS spectrum with a series of Mn^{IV} coordination compound spectra suggests that the electronic structure of Mn in the S_3 state is much more similar to $salpn_2Mn_2^{IV}(OH)_2$ (Fig. 1b) rather than $salpn_2Mn_2^{IV}O_2$ (Fig. 1d), $phen_4Mn_2^{IV}O_2$ complex (Fig. 1e), $Mn_3^{IV}O_4$ Acbpy (Fig. 1g) or the oxide $Mn^{IV}O_2$ (Fig. 1h).

The OEC goes through four redox states during the S_0 to S_3 state transitions. Our study shows that the RIXS spectral changes in PS II are considerably weaker than the changes observed within the Mn^{IV} coordination complexes. They are also weaker than the spectral changes between Mn oxides. We, therefore, conclude that redox reactions of the OEC must be considered within the entire Mn_4CaO_5 entity. Namely, the ligands participate in the charge balancing. A description of the electronic structure at the Mn sites thus has to go beyond the assignment of formal oxidation states. We note that this does not contradict other studies such as EPR and ENDOR, because a different response is probed in the various techniques.

We have shown that the formal oxidation states may be insufficient for describing the complex nature of the electronic structure in multinuclear clusters like the Mn₄CaO₅ cluster in PS II. Electrons are strongly delocalized in the Mn₄CaO₅ cluster, and ligands may be intimately involved in the redox chemistry. As a consequence, the Mn RIXS spectral changes are subtle during the S-state transitions. Of the two main mechanisms that are being considered for the O-O bond formation catalyzed by the OEC, one involves the generation of a Mn^V-oxo group in the final step when the O-O bond is formed, and the alternate mechanism involves delocalization of the charge onto a ligand and the subsequent chemistry of O-O bond formation. 6b, 11 The current results show that the change of the electronic charge includes the ligands in all S-state transitions. Therefore, the mechanisms that rely on delocalization of charge on the ligands may become more relevant, and any proposed mechanism requires one to take this into account. Moreover, this suggests that such delocalization may play a role during the O-O bond formation step in the S₄ state.

Supplementary Material

Refer to Web version on PubMed Central for supplementary material.

Acknowledgments

This work was supported by the NIH grant (GM 55302), and the DOE, Director, Office of Science, Office of Basic Energy Sciences (OBES), Chemical Sciences, Geosciences, and Biosciences Division, under Contract DE-AC02-05CH11231. Parts of this research were carried out at ESRF, APS, and SSRL operated by Stanford University for DOE, OBES. We thank Dr. Sumit Bhaduri for providing model complexes.

ABBREVIATIONS

RIXS Resonant Inelastic X-ray Scattering
XAS X-ray Absorption Spectroscopy
PS II Photosystem II

OEC Oxygen Evolving Complex

References

- 1. Wydrzynski, T.; Satoh, S. Photosystem II: The Light-Driven Water:Plastoquinone Oxidoreductase. Springer; Dordrecht: 2005.
- 2. Messinger J. Phys Chem Chem Phys. 2004; 6:4764–4771.
- (a) Kulik LV, Epel B, Lubitz W, Messinger J. J Am Chem Soc. 2005; 127:2392–2393. [PubMed: 15724984]
 (b) Kulik LV, Epel B, Lubitz W, Messinger J. J Am Chem Soc. 2007; 129:13421–13435. [PubMed: 17927172]
- Iuzzolino L, Dittmer J, Dörner W, Meyer-Klaucke W, Dau H. Biochemistry. 1998; 37:17112– 17119. [PubMed: 9860823]
- 5. Messinger J, Robblee JH, Bergmann U, Fernandez C, Glatzel P, Visser H, Cinco RM, McFarlane KL, Bellacchio E, Pizarro SA, Cramer SP, Sauer K, Klein MP, Yachandra VK. J Am Chem Soc. 2001; 123:7804–7820. [PubMed: 11493054]
- 6. (a) McEvoy JP, Brudvig GW. Chem Rev. 2006; 106:4455–4483. [PubMed: 17091926] (b) Siegbahn PEM. Acc Chem Res. 2009; 42:1871–1880. [PubMed: 19856959] (c) Yamanaka S, Isobe H, Kanda K, Saito T, Umena Y, Kawakami K, Shen JR, Kamiya N, Okumura M, Nakamura H, Yamaguchi K. Chem Phys Lett. 2011; 511:138–145.(d) Saito T, Yamanaka S, Kanda K, Isobe H, Takano Y, Shigeta Y, Umena Y, Kawakami K, Shen JR, Kamiya N, Okumura M, Shoji M, Yoshioka Y, Yamaguchi K. Int J Quantum Chem. 2012; 112:253–276.(e) Kolling DRJ, Cox N, Ananyev GM, Pace RJ, Dismukes GC. Biophys J. 2012; 103:313–322. [PubMed: 22853909]
- 7. Glatzel P, Bergmann U, Yano J, Visser H, Robblee JH, Gu WW, de Groot FMF, Christou G, Pecoraro VL, Cramer SP, Yachandra VK. J Am Chem Soc. 2004; 126:9946–9959. [PubMed: 15303869]
- 8. (a) Westre TE, Kennepohl P, DeWitt JG, Hedman B, Hodgson KO, Solomon EI. J Am Chem Soc. 1997; 119:6297–6314.(b) de Groot F, Vanko G, Glatzel P. J Phys-Condens Mat. 2009; 21
- (a) Baldwin MJ, Stemmler TL, Riggsgelasco PJ, Kirk ML, Pennerhahn JE, Pecoraro VL. J Am Chem Soc. 1994; 116:11349–11356.(b) Mukherjee S, Stull JA, Yano J, Stamatatos TC, Pringouri K, Stich TA, Abboud KA, Britt RD, Yachandra VK, Christou G. Proc Natl Acad Sci USA. 2012; 109:2257–2262. [PubMed: 22308383]
- Messinger J, Robblee JH, Yu WO, Sauer K, Yachandra VK, Klein MP. J Am Chem Soc. 1997; 119:11349–11350.
- 11. Cady CW, Crabtree RH, Brudvig GW. Coord Chem Rev. 2008; 252:444–455. [PubMed: 21037800]

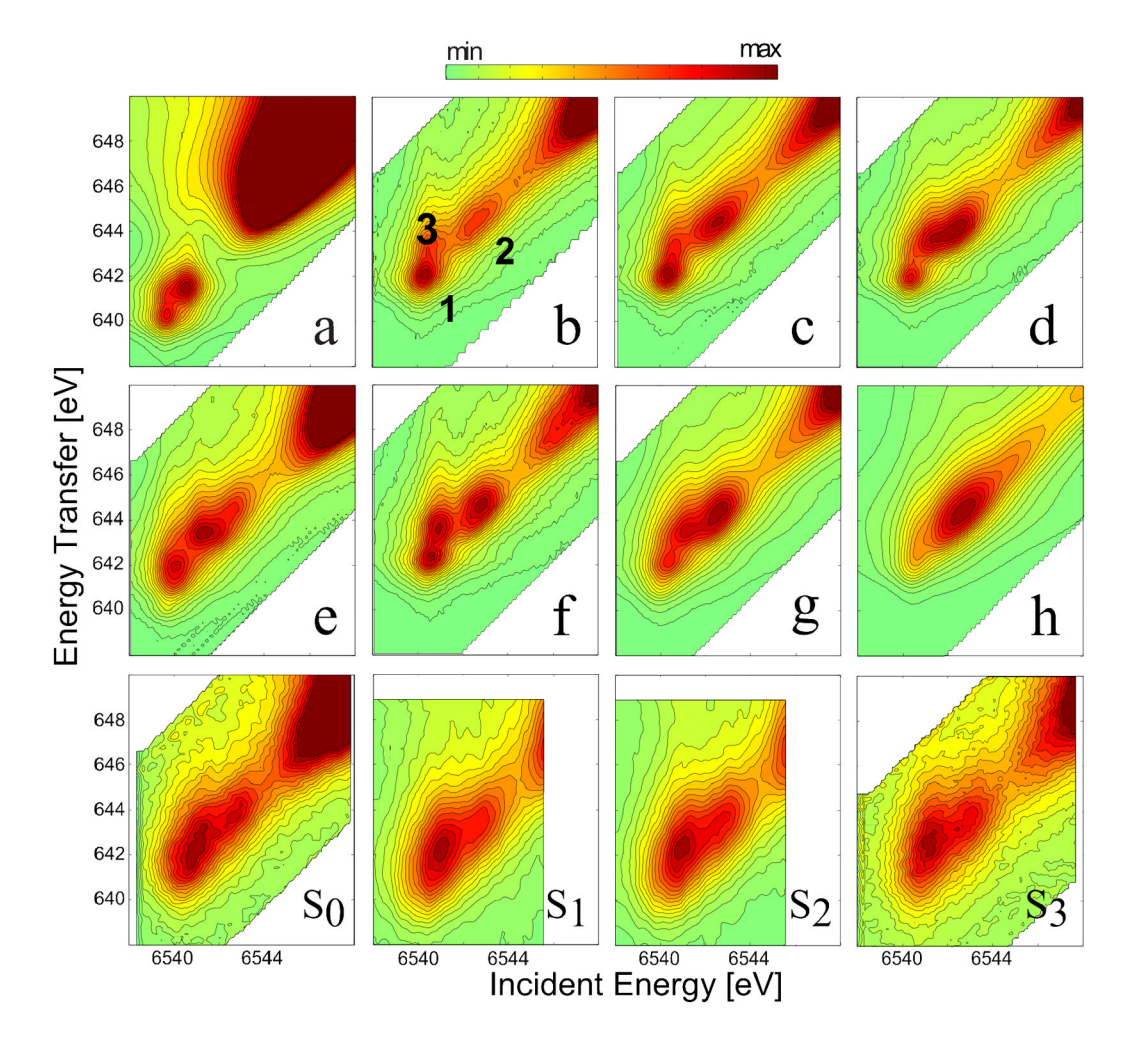


Figure 1. Contour plots of Mn 1s2p RIXS planes of model compounds and the OEC in PS II in the S_0 to S_3 states. (a) $Mn^{II}O$, (b) $salpn_2Mn^{IV}_2(OH)_2$, (c) $salpn_2Mn^{IV}_2(O)(OH)$, (d) $salpn_2Mn^{IV}_2(O)_2$, (e) $phen_4Mn^{IV}_2(O)_2$, (f) $Mn^{IV}_3Ca_2$, (g) $Mn^{IV}_3(O)_4Acbpy$, (h) $Mn^{IV}_3Ca_2$. The energy axes are identical for all spectra. The intensity is normalized to the maximum in the pre-edge region. for all spectra.

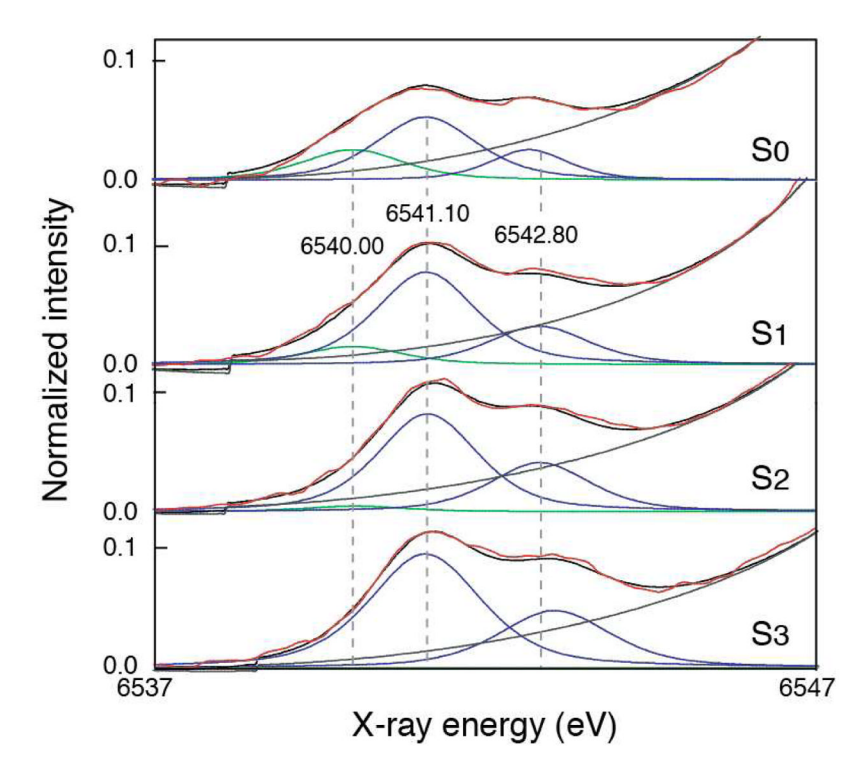
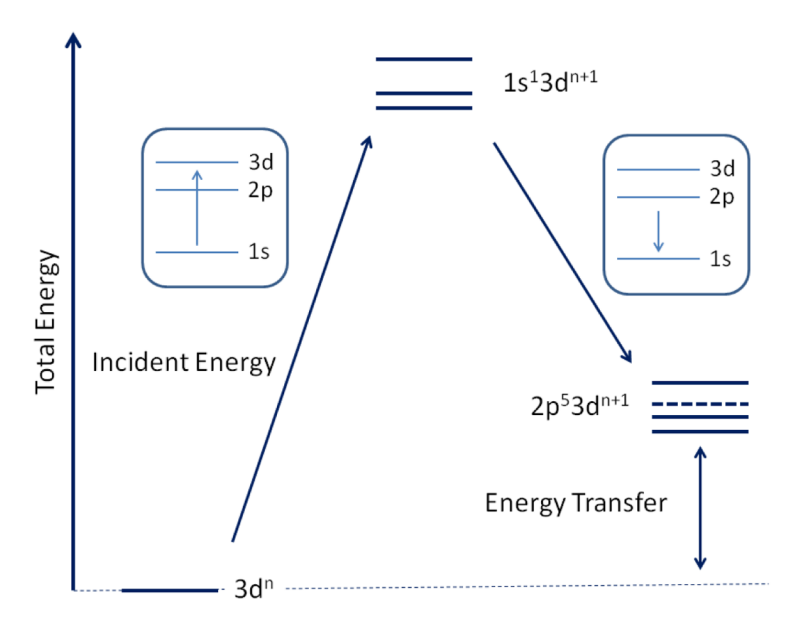


Figure 2. K absorption pre-edges and fit of Mn in PS II (red, experimental data; black, fit; blue and green, peak components; gray, background). The dashed lines are guides to the eye.



Scheme 1.

Total energy diagram for the 1s2p RIXS process. The fine splitting of the states in the intermediate and final state is indicated. The dashed line represents a final state that arises from 2p3d interactions that are absent in the intermediate state..